The EMBO Journal Vol. 21 No. 19 pp. 5195–5205, 2002

Chk2-deficient mice exhibit radioresistance and defective p53-mediated transcription

Hiroyuki Takai[1,2], Kazuhito Naka[1], Yuki Okada[3,4], Miho Watanabe[5], Naoki Harada[5], Shin'ichi Saito[6,7], Carl W.Anderson[8], Ettore Appella[6], Makoto Nakanishi[9], Hiroshi Suzuki[5], Kazuo Nagashima[3,4], Hirofumi Sawa[3,4], Kyoji Ikeda[1] and Noboru Motoyama[1,10]

[1]Department of Geriatric Research, National Institute for Longevity Sciences (NILS), Obu, Aichi 474-8522, [3]Laboratory of Molecular and Cellular Pathology, Hokkaido University Graduate School of Medicine, [4]CREST, JST, Sapporo 060-8638, [5]Research Laboratories, Chugai Pharmaceutical Co. Ltd, Gotennba, Shizuoka 412-8513, [9]Department of Biochemistry, Nagoya City University Medical School, Nagoya 467-8601, Japan, [6]Laboratory of Cell Biology, National Cancer Institute, National Institutes of Health, Bethesda, MD 20892 and [8]Biology Department, Brookhaven National Laboratory, Upton, NY 11973, USA

[2]Present address: Laboratory of Cell Biology and Genetics, The Rockefeller University, New York, NY 10021, USA
[7]Present address: Gene Response Section, National Cancer Institute, National Institutes of Health, Bethesda, MD 20892, USA

[10]Corresponding author
e-mail: motoyama@nils.go.jp

H.Takai and K.Naka contributed equally to this work

The mammalian Chk2 kinase is thought to mediate ATM-dependent signaling in response to DNA damage. The physiological role of mammalian Chk2 has now been investigated by the generation of Chk2-deficient mice. Although *Chk2*$^{-/-}$ mice appeared normal, they were resistant to ionizing radiation (IR) as a result of the preservation of splenic lymphocytes. Thymocytes and neurons of the developing brain were also resistant to IR-induced apoptosis. The IR-induced G_1/S cell cycle checkpoint, but not the G_2/M or S phase checkpoints, was impaired in embryonic fibroblasts derived from *Chk2*$^{-/-}$ mice. IR-induced stabilization of p53 in *Chk2*$^{-/-}$ cells was 50–70% of that in wild-type cells. Caffeine further reduced p53 accumulation, suggesting the existence of an ATM/ATR-dependent but Chk2-independent pathway for p53 stabilization. In spite of p53 protein stabilization and phosphorylation of Ser23, p53-dependent transcriptional induction of target genes, such as p21 and Noxa, was not observed in *Chk2*$^{-/-}$ cells. Our results show that Chk2 plays a critical role in p53 function in response to IR by regulating its transcriptional activity as well as its stability.

Keywords: ataxia-telangiectasia mutated (ATM)/cell cycle checkpoint/DNA damage/phosphorylation/transcriptional activation

Introduction

Disruption of the mechanisms in multicellular organisms that regulate checkpoint and apoptotic responses leads to genomic instability and the development of cancer. Several protein kinases play key roles in the activation of these pathways in response to DNA damage including ataxia-telangiectasia-mutated (ATM) defects that result in ataxia telangiectasia, ATR (ATM and rad3-related) and their kinase substrates Chk2 and Chk1 (Giaccia and Kastan, 1998; Appella and Anderson, 2001). Mammalian Chk1 is essential for early embryonic development and the G_2 checkpoint response to DNA damage and replication block (Liu *et al*., 2000; Takai *et al*., 2000). Chk2, the mammalian homolog of the *Saccharomyces cerevisiae* Rad53 and *Schizosaccharomyces pombe* Cds1 kinases, also is implicated in the DNA damage signaling pathway (Bartek *et al*., 2001). Chk2 is activated by phosphorylation in an ATM-dependent manner in response to ionizing radiation (IR), and in an ATM-independent manner in response to UV radiation or stalled DNA replication. Activated Chk2 phosphorylates Cdc25A on serine (Ser)123, Cdc25C on Ser215, BRCA1 on Ser988, and p53 on several sites including Ser20 (Bartek *et al*., 2001). Recently, heterozygous germline mutations in the human *Chk2* gene were found in a subset of patients with Li–Fraumeni syndrome (Bell *et al*., 1999). Most cases of this highly penetrant familial cancer syndrome result from inheritance of a mutant *p53* allele and the subsequent somatic loss of the remaining wild-type allele.

The p53 tumor suppressor protein plays a central role in a cells' decision to induce either cell cycle arrest or apoptosis after diverse stresses, including DNA damage, hypoxia and the activation of oncogenes (Giaccia and Kastan, 1998; Prives and Hall, 1999; Vousden, 2000). Regulation of the abundance and transcriptional activity of p53 is achieved primarily by post-translational modifications, such as phosphorylation and acetylation (Appella and Anderson, 2001). In normal cells p53 protein levels are low due to Mdm2-mediated ubiquitylation and degradation through the proteasome pathway. Mdm2 may also regulate p53 activity by facilitating nuclear export and degradation following ubiquitylation (Liang and Clarke, 2001). In response to stress such as IR, human p53 is phosphorylated at several sites in its transactivation domain including Ser15 and Ser20. ATM phosphorylates p53 on Ser15 (Banin *et al*., 1998; Canman *et al*., 1998), and this phosphorylation was suggested to inhibit the interaction of p53 with Mdm2, resulting in p53 stabilization (Shieh *et al*., 1997; Chehab *et al*., 1999). ATM-dependent phosphorylation of Mdm2 reduces its capability to promote nucleo-cytoplasmic shuttling and the subsequent degradation of p53 (Maya *et al*., 2001).

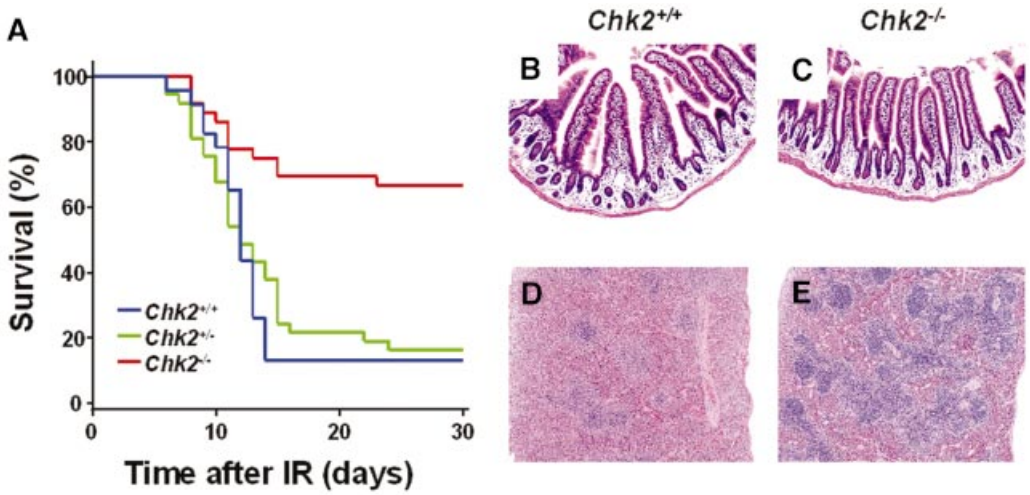

Fig. 1. Reduced radiosensitivity of $Chk2^{-/-}$ mice and $Chk2^{-/-}$ splenocytes *in vivo*. (**A**) Kaplan–Meier survival curve of age-matched 8–16-week-old $Chk2^{+/+}$ (n = 23), $Chk2^{+/-}$ (n = 37) and $Chk2^{-/-}$ (n = 36) mice after exposure to 8 Gy of X-rays. Data are combined from two separate experiments. (**B** and **C**) Normal appearance of intestine in $Chk2^{+/+}$ (B) and $Chk2^{-/-}$ (C) mice 1 day after IR. (**D** and **E**) Atrophy of white pulp of the spleen and reduction of splenocyte number in $Chk2^{+/+}$ mice (D), but not in $Chk2^{-/-}$ mice (E), 8 days after exposure to IR.

Transcriptional activation of p53 also is regulated by acetylation at several C-terminal lysine (Lys) residues by CBP/p300 and PCAF (Appella and Anderson, 2001). Acetylation is believed to activate the sequence-specific DNA binding ability of p53, which is required for most, if not all, p53-mediated responses (Ito *et al*., 2001). Data from mutants indicate that acetylation is induced by phosphorylation of sites in the N-terminal transactivation domain of p53, including Ser15, which is thought to recruit CBP/p300 to p53. In addition, ATM was shown to activate Chk2, which phosphorylates several N-terminal p53 sites including Ser20, and these phosphorylations also may contribute to both stabilization and transcriptional activation of the p53 protein (Chehab *et al*., 2000; Hirao *et al*., 2000; Shieh *et al*., 2000). The extent to which Chk2 participates in p53 stabilization and activation in response to DNA damage, such as that induced by IR, remains unclear, however.

To characterize the function of Chk2, we generated Chk2-deficient ($Chk2^{-/-}$) mice. We now show that, in contrast to Chk1-deficient ($Chk1^{-/-}$) mice (Liu *et al*., 2000; Takai *et al*., 2000), $Chk2^{-/-}$ mice are viable and fertile. Moreover, $Chk2^{-/-}$ mice were more resistant than $Chk2^{+/+}$ mice to sublethal doses of IR. Partial stabilization of the p53 protein was observed in $Chk2^{-/-}$ cells in response to IR; however, even though phosphorylation and acetylation of p53 after IR were apparently normal, the transcriptional activity of p53 was abolished. Thus, Chk2 plays a pivotal role in the biological activity of p53 by regulating its transcriptional activation as well as its stabilization after IR-induced damage.

Results

Inactivation of the Chk2 gene in mice

We generated $Chk2^{-/-}$ mice by gene targeting in embryonic stem (ES) cells (see Supplementary data available at *The EMBO Journal* Online). $Chk2^{-/-}$ animals were born in the expected ratio and appeared normal. Three of 34 $Chk2^{-/-}$ mice, one of 23 $Chk2^{+/-}$ mice and none of 22 $Chk2^{+/+}$ mice were dead by 1 year. One of the $Chk2^{-/-}$ mice that died developed a mammary gland epithelial tumor (data not shown).

Increased survival of $Chk2^{-/-}$ mice upon IR

Chk2 is phosphorylated and activated by ATM in response to IR (Bartek *et al*., 2001). Given that $Atm^{-/-}$ mice manifest extreme sensitivity to IR (Barlow *et al*., 1996), we examined whether Chk2 deficiency also results in acute radiation toxicity. Eight to 16-week-old $Chk2^{+/+}$, $Chk2^{+/-}$ and $Chk2^{-/-}$ mice were exposed to a sublethal dose (8 Gy) of IR and then monitored for survival and illness. Both $Chk2^{+/+}$ and $Chk2^{+/-}$ mice began to die from 6 days after IR, and more than two-thirds of these animals died within 2 weeks after IR. In sharp contrast, $Chk2^{-/-}$ mice were resistant to IR, and approximately two-thirds survived beyond 30 days after IR exposure (Figure 1A). The 50% survival times for $Chk2^{+/+}$, $Chk2^{+/-}$ and $Chk2^{-/-}$ mice were 12 ± 0.5 days (means ± standard deviation), 13 ± 1.5 days and >30 days, respectively. Kaplan–Meier survival analysis revealed that the prolongation of survival in $Chk2^{-/-}$ mice was statistically significant ($P < 0.0001$) compared with $Chk2^{+/+}$ and $Chk2^{+/-}$ mice. Although $Atm^{-/-}$ mice die within 3–5 days post-irradiation as a result of acute radiation toxicity to the gastrointestinal tract, with epithelial crypt degeneration and abscess formation (Barlow *et al*., 1996), $Chk2^{-/-}$ mice did not exhibit any pathological abnormalities in the esophagus, stomach and small or large intestines when compared with $Chk2^{+/+}$ mice after IR (Figure 1B and C). The time of death in $Chk2^{+/+}$ mice, between 1 and 2 weeks after irradiation, is consistent with the kinetics of lymphocyte depletion and resulting infection, suggesting that Chk2 deficiency might render lymphocytes radioresistant. To evaluate this hypothesis, we performed histological analysis of the spleen after IR. Marked atrophy of, and a reduced number of, lymphocytes in the white pulps were apparent in the spleens of $Chk2^{+/+}$ and $Chk2^{+/-}$ mice 8 days after IR (Figure 1D; data not shown). In contrast, no such changes were detected in $Chk2^{-/-}$ mice (Figure 1E). These results

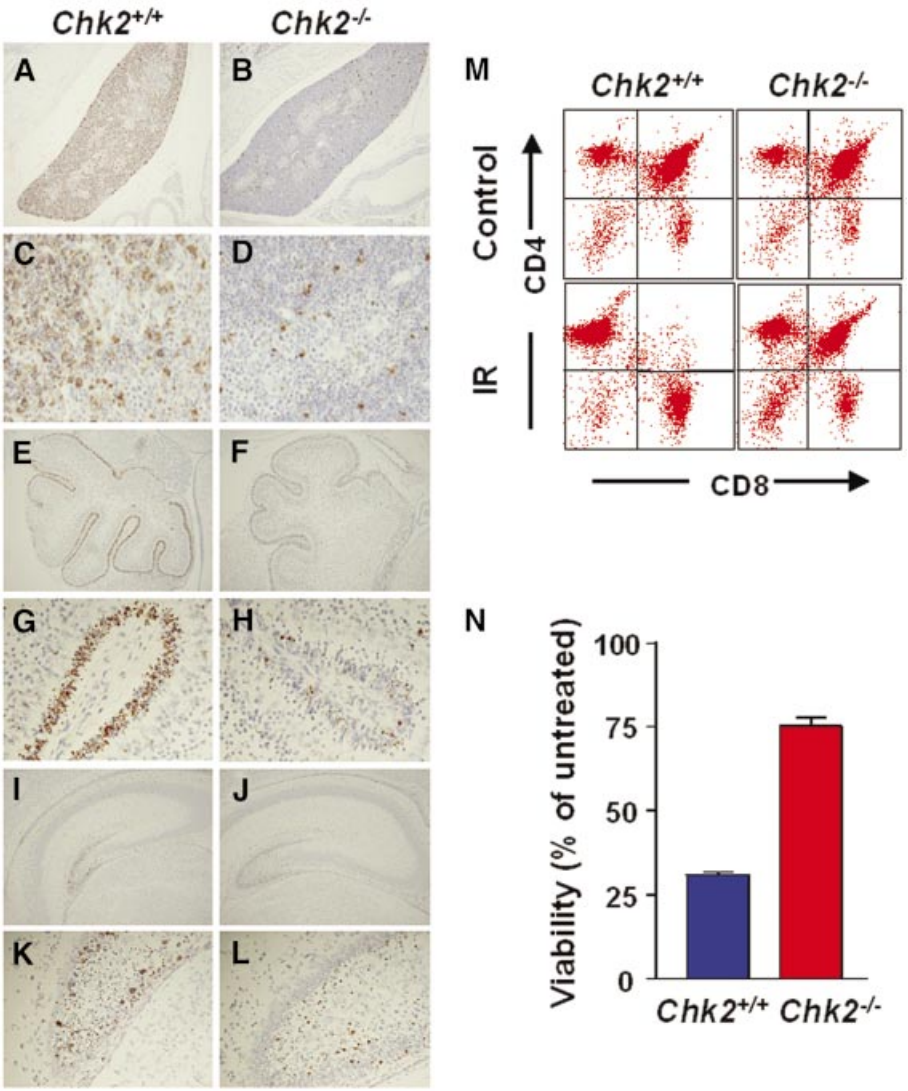

Fig. 2. Defective IR-induced apoptosis in the thymus and developing brain of *Chk2*$^{-/-}$ mice. (**A**–**D**) TUNEL staining of thymi derived from 2- to 3-month-old *Chk2*$^{+/+}$ (A and C) and *Chk2*$^{-/-}$ (B and D) mice 9 h after exposure to 8 Gy of IR. Magnification: 4× (A and B) or 40× (C and D). (**E**–**L**) TUNEL staining of the cerebellum from *Chk2*$^{+/+}$ (E and G), *Chk2*$^{-/-}$ (F and H) mice and of the hippocampus from *Chk2*$^{+/+}$ (I and K) and *Chk2*$^{-/-}$ (J and L) mice at 4 days of age and 9 h after exposure to 8 Gy of IR. Magnification: 10× (E, F, I and J) or 40× (G, H, K and L). (**M**) Flow cytometric analysis of thymocytes isolated from control *Chk2*$^{+/+}$ and *Chk2*$^{-/-}$ mice or from irradiated animals 24 h after exposure to 4 Gy of IR. The cells were stained for CD4 and CD8. (**N**) Sensitivity of isolated thymocytes to IR. Thymocytes derived from *Chk2*$^{+/+}$ and *Chk2*$^{-/-}$ mice were exposed to 4 Gy of IR and cultured for 24 h before determining viability by staining with propidium iodide and flow cytometry. Data are expressed as a percentage of the viability of the corresponding non-irradiated cells and are means ± standard deviation from three independent experiments.

indicate that lymphocytes in the spleens of *Chk2*$^{-/-}$ mice are resistant to IR, rendering the mice themselves radioresistant also.

Decreased cell death in response to IR in Chk2$^{-/-}$ *mice*

The resistance of *Chk2*$^{-/-}$ splenocytes to IR suggests that Chk2 might be involved in the apoptotic pathway *in vivo*. Both immature thymocytes and neurons in the developing CNS are susceptible to IR-induced apoptosis (Clarke *et al*., 1993; Lowe *et al*., 1993; Herzog *et al*., 1998). To examine the role of Chk2 in the apoptotic response, we examined the thymus and developing brain of *Chk2*$^{-/-}$ mice by TUNEL analysis. Although whole body irradiation resulted in widespread apoptosis in the cortical region of the thymus in *Chk2*$^{+/+}$ mice (Figure 2A and C), apoptotic cells were rarely detected in the thymus of *Chk2*$^{-/-}$ mice (Figure 2B and D). Flow cytometric analysis of thymocytes isolated from mice subjected (or not) to IR revealed that CD4 and CD8 double-positive cells from *Chk2*$^{+/+}$ mice were highly sensitive to IR, whereas such double-positive thymocytes from *Chk2*$^{-/-}$ mice were resistant to IR-induced apoptosis (Figure 2M). Consistent with these *in vivo* observations, *Chk2*$^{-/-}$ thymocytes irradiated *in vitro* also were resistant to IR-induced apoptosis (Figure 2N). In the developing CNS of *Chk2*$^{+/+}$ mice, neurons in the external germinal layer of the cerebellum and in the dentate gyrus of the hippocampus exhibited widespread apoptotic death in response to IR (Figure 2E, G, I and K). In contrast, neurons in the same regions of the CNS of

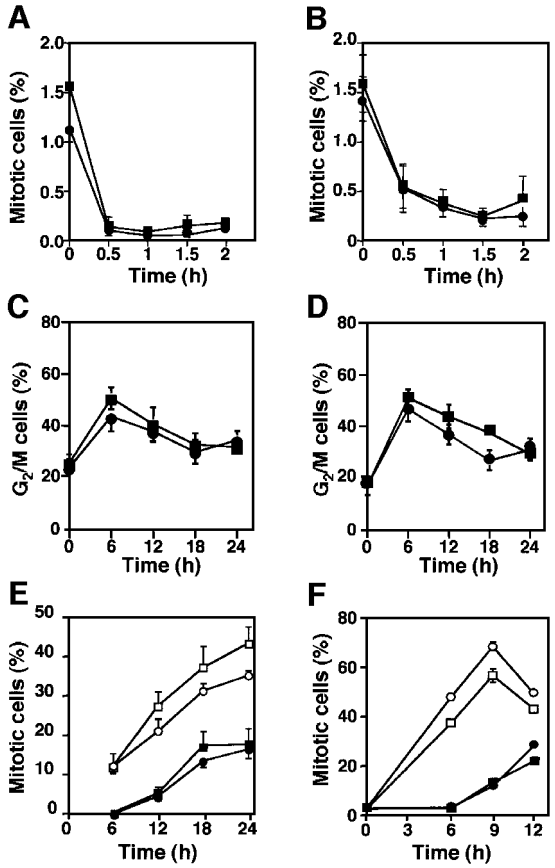

Fig. 3. Normal G_2/M checkpoint activation in *Chk2*$^{-/-}$ mice. (**A** and **B**) Activation of the G_2/M checkpoint. Mitotic index of irradiated or unirradiated *Chk2*$^{+/+}$ (squares) and *Chk2*$^{-/-}$ (circles) MEFs (A) and ES cells (B) was determined at the indicated times after 10 Gy IR. Data are expressed as the percentage of mitotic cells of total cells; means ± standard deviation are from triplicate experiments. (**C** and **D**) The fraction of G_2/M *Chk2*$^{+/+}$ (squares) or *Chk2*$^{-/-}$ (circles) MEFs (C) or ES cells (D) was determined at the indicated times after 10 Gy IR. The means ± standard deviation from three independent experiments are given. (**E** and **F**) Maintenance of the G_2/M checkpoint. Irradiated (closed symbols) and unirradiated (open symbols) *Chk2*$^{+/+}$ (squares) and *Chk2*$^{-/-}$ (circles) MEFs (E) and ES cells (F) were treated with 0.2 μg/ml nocodazole, and the percentage of mitotic cells was determined at the indicated times after 10 Gy IR. Means ± standard deviation from replicate (n = 4) (E) or triplicate (F) experiments are given.

Chk2$^{-/-}$ mice were resistant to IR-induced apoptosis (Figure 2F, H, J and L). These results indicate that Chk2 mediates IR-induced apoptosis in thymocytes and in neurons of the developing CNS.

Cell cycle checkpoint in Chk2-deficent cells

To examine the role of Chk2 in cell cycle checkpoint responses to IR, cells were irradiated and then mitotic indexes were determined. Within 0.5 h of exposure to IR, the mitotic index had significantly decreased (Figure 3A and B), and the cells accumulated in G_2/M, reaching a peak at 6 h, after which the index decreased for both MEFs and ES cells from *Chk2*$^{+/+}$ and *Chk2*$^{-/-}$ mice (Figure 3C and D). To examine maintenance of the G_2 checkpoint, irradiated or non-irradiated cells were treated with nocodazole, which traps cells in mitosis, and the mitotic index was then determined at various times. The mitotic index of both non-irradiated *Chk2*$^{+/+}$ and *Chk2*$^{-/-}$ MEFs and ES cells increased with time. In response to IR, both *Chk2*$^{+/+}$ and *Chk2*$^{-/-}$ MEFs and ES cells arrested in G_2 for 6 h, after which the proportion of mitotic cells of both genotypes gradually increased with similar kinetics (Figure 3E and F). These data indicate that both the initiation and maintenance of the G_2 checkpoint are normal in *Chk2*$^{-/-}$ MEFs and ES cells.

To examine the G_1/S checkpoint in *Chk2*$^{-/-}$ MEFs, asynchronous MEFs were irradiated and the numbers of cells in G_1, S and G_2/M were determined by FACS analysis as shown in Figure 4A. For early time points after IR (up to 2 h), the number of S phase cells was the same for both *Chk2*$^{+/+}$ and *Chk2*$^{-/-}$ MEFs (Figure 4B). However, from 4 h after IR, the decrease in the number of *Chk2*$^{-/-}$ S phase MEFs was smaller than that for *Chk2*$^{+/+}$ MEFs (Figure 4B). To examine maintenance of the G_1 checkpoint at later times, asynchronous MEFs were treated with nocodazole with or without IR, and then the DNA content was determined as shown in Figure 4C. At 18 and 24 h after IR, the fraction of *Chk2*$^{+/+}$ MEFs in the G_1 phase was increased, whereas that of *Chk2*$^{-/-}$ MEFs was not (Figure 4C and D). Finally, serum-starved MEF cells were irradiated (or not) and then stimulated to enter the cycle by the addition of serum. BrdU was also added to the incubation medium to allow the detection of cells entering S phase. Cells were harvested 24 h after stimulation and the number of cells that entered S phase was determined by flow cytometry. Whereas irradiation reduced the proportion of *Chk2*$^{+/+}$ cells in S phase by 52%, it reduced the proportion of *Chk2*$^{-/-}$cells that had entered S phase by only 25% (Figure 4E). As initiation and maintenance of the G_1 checkpoint are regulated, in part, through inhibition of cyclin E-associated Cdk2 activity (Bartek *et al*., 2001), we examined whether Chk2 deficiency affected this kinase activity after IR. Consistent with our FACS data, cyclin E-associated Cdk2 activities were decreased in both *Chk2*$^{+/+}$ and *Chk2*$^{-/-}$ MEFs in response to IR (Figure 4G and H); however, in *Chk2*$^{-/-}$ MEFs, its activities again increased by 2.5 h after exposure to IR (Figure 4H). Together, these results show that initiation of the G_1 arrest in response to IR, which is independent of p53, is intact, but maintenance of the G_1 arrest beyond 2 h, which is dependent on p53, is defective in *Chk2*$^{-/-}$ MEFs.

ATM-deficient cells undergo radioresistant DNA synthesis (RDS), indicating a defect in IR-induced S phase arrest (Rotman and Shiloh, 1999; Kastan and Lim, 2000). Chk2 phosphorylates Cdc25A in response to IR, inducing its degradation and inhibition of cyclin E-associated Cdk2 kinase activity, which results in S phase arrest (Bartek *et al*., 2001). To examine the S phase checkpoint in *Chk2*$^{-/-}$ MEFs, thymidine incorporation was determined in asynchronous MEFs irradiated with X-rays from 4–20 Gy. While inhibition of DNA synthesis did take place in the absence of Chk2, a subtle difference was observed between *Chk2*$^{+/+}$ and *Chk2*$^{-/-}$ MEFs (Figure 4F). Accordingly, inhibition of cyclin E-associated Cdk2 activities was observed in both *Chk2*$^{+/+}$ and *Chk2*$^{-/-}$ MEFs in response to IR (Figure 4G and H). These results indicate that, while Chk2 may play some role in regulating S phase progression, it is dispensable for the overall activation of the S phase checkpoint after IR.

Stabilization of p53 protein in Chk2$^{-/-}$ cells after IR

The abnormalities in apoptosis and cell cycle checkpoint control in *Chk2*$^{-/-}$ cells are suggestive of a functional interaction between Chk2 and p53. To better define the role played by Chk2 in p53 stabilization, we analyzed p53 protein levels in *Chk2*$^{-/-}$ thymocytes, MEFs and ES cells following DNA damage. Consistent with previous observations (Clarke *et al*., 1993; Lowe *et al*., 1993), IR induced a marked increase in the amount of p53 in *Chk2*$^{+/+}$ thymocytes that was apparent within 1 h (Figure 5A). Accumulation of p53 also was detected in *Chk2*$^{-/-}$ thymocytes, although the maximum level was only 50–70% of that apparent in *Chk2*$^{+/+}$ thymocytes (Figure 5A and B). Similar results were obtained with MEFs (Figure 5C) and ES cells (Figure 5D). Stable expression of human Chk2 in *Chk2*$^{-/-}$ ES cells restored IR-induced stabilization of p53 to the level apparent in *Chk2*$^{+/+}$ ES cells (Figure 5D). These results indicate that Chk2 contributes to the stabilization of p53 induced by IR *in vivo*. The partial nature of the defect in IR-induced p53 stabilization observed in Chk2-deficient cells suggested the existence of an alternative pathway for p53 stabilization. We therefore examined whether ATM or ATR contribute to p53 stabilization in *Chk2*$^{-/-}$ cells by investigating the effect of caffeine, a known inhibitor of ATM and ATR (Sarkaria *et al*., 1999). The extent of IR-induced stabilization of p53 in both *Chk2*$^{-/-}$ and *Chk2*$^{+/+}$ cells was markedly reduced by caffeine (Figure 5E), suggesting that p53 stabilization in *Chk2*$^{-/-}$ cells is mediated by the ATM or ATR pathways. One of the major downstream effectors of ATR is Chk1 (Liu *et al*., 2000); thus, we examined the activation of Chk1 after IR. Chk1 exhibited a lower electrophoretic mobility and increased phosphorylation on Ser345 in response to either IR or UV in both *Chk2*$^{+/+}$ and *Chk2*$^{-/-}$ MEFs, but the changes were weaker in response to IR (Figure 5F). These results indicate that Chk1 is activated in response to both types of DNA damage, and that Chk1 may be involved in the regulation of p53 stabilization and function in *Chk2*$^{-/-}$ cells.

Defective transcriptional activation of p53 protein in Chk2$^{-/-}$ cells

The p53 protein regulates the expression of many genes whose products play important roles in cell cycle arrest and apoptosis. In this work we examined the expression of several known p53 target genes, including *Mdm2*, *Cdkn1a* (p21), *Pmaip1* (Noxa), *Ccng* (cyclin G1) and *Bax*, in thymocytes and MEFs using real-time, quantitative RT–PCR. Messenger RNAs for *Mdm2*, *Cdkn1a*, *Pmaip1* and *Bax* were significantly induced with a peak at 4–6 h after IR in *Chk2*$^{+/+}$ thymocytes, however, none of these mRNAs accumulated after IR-treatment in *Chk2*$^{-/-}$

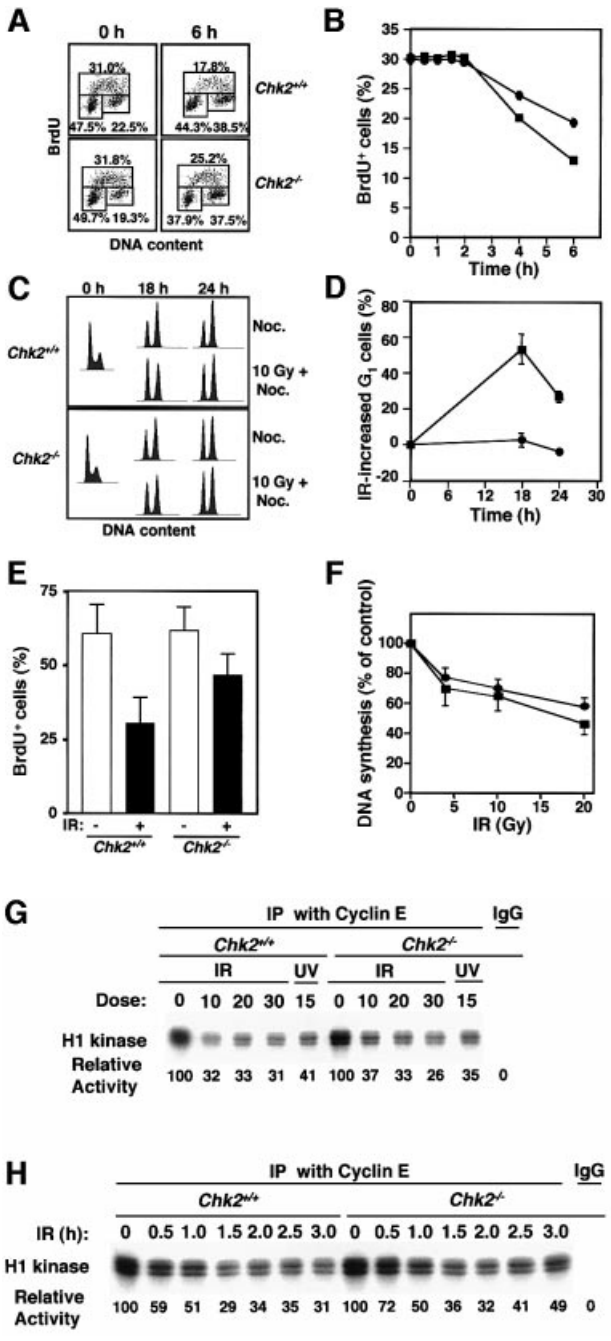

Fig. 4. Defective G_1, but not S phase, checkpoint activation in *Chk2*$^{-/-}$ mice. (**A**) Representative data of dot-plots of BrdU fluorescence versus DNA content for *Chk2*$^{+/+}$ or *Chk2*$^{-/-}$ MEFs at the times indicated after 10 Gy IR. Irradiated and unirradiated MEFs were treated with 10 μM BrdU for 30 min before cells were harvested and analyzed by flow cytometry. (**B**) The percentage of total cells that were BrdU positive from *Chk2*$^{+/+}$ (squares) or *Chk2*$^{-/-}$ (circles) MEFs as described in (A); the means ± standard deviation are from triplicate experiments. (**C**) Representative histograms show DNA content of *Chk2*$^{+/+}$ or *Chk2*$^{-/-}$ MEFs at the times indicated after 10 Gy IR. Cells were treated with 1 mg/ml nocodazole, and at the indicated time points after IR, they were harvested and analyzed by flow cytometry. (**D**) A summary of triplicate experiments as described in (C). The percentage increase in G_1 is the difference in the percent G_1 content between irradiated and unirradiated *Chk2*$^{+/+}$ (squares) or *Chk2*$^{-/-}$ (circles) control cells, respectively. (**E**) Defective ability of *Chk2*$^{-/-}$ MEFs to block S phase entry following 20 Gy IR. Serum-starved MEFs were released from G_1 arrest into complete medium containing BrdU (65 μM) and immediately subjected (or not) to irradiation. Cells were harvested 24 h after release and the number of BrdU positive cells was determined as a percentage of total cells by flow cytometry. Data are means ± standard deviation of values from replicate experiments ($n = 4$). (**F**) Normal S phase checkpoint activation in *Chk2*$^{-/-}$ MEFs. Replicative DNA synthesis was assessed 1 h after the indicated doses of IR in *Chk2*$^{+/+}$ (squares) or *Chk2*$^{-/-}$ (circles) MEFs. (**G** and **H**) The activity of cyclin E-associated Cdk2 at 2 h after IR at the indicated dose (Gy) or after 15 J/m^2 UV and (G) at the times indicated after IR (20 Gy) (H). Relative kinase activities are indicated at the bottom.

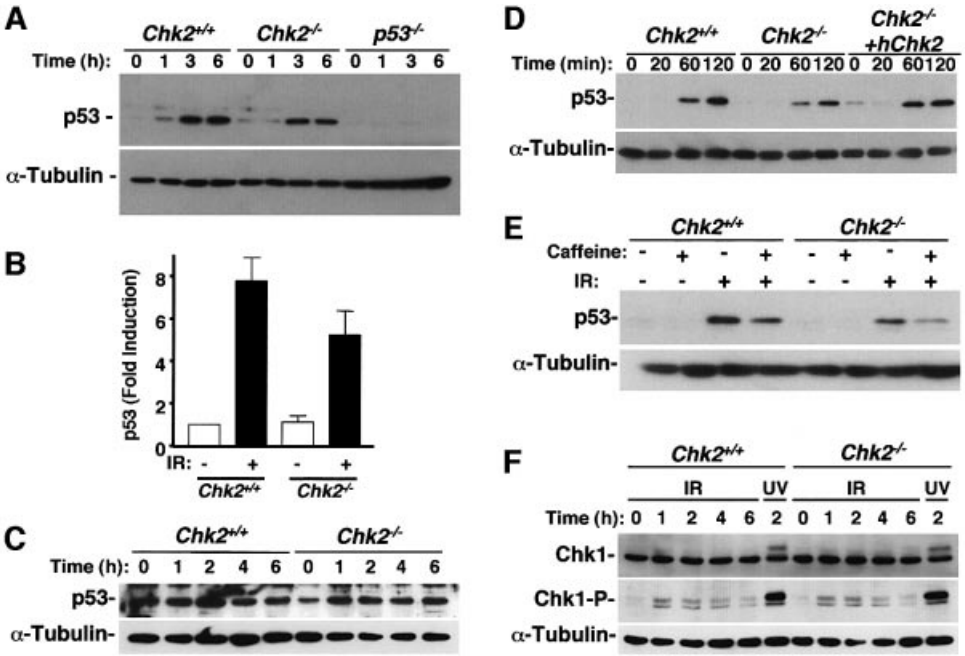

Fig. 5. IR-induced stabilization of p53 in *Chk2*$^{-/-}$ thymocytes, MEFs and ES cells. (**A**) Immunoblot analysis of the time course of p53 abundance after exposure of thymocytes from *Chk2*$^{+/+}$, *Chk2*$^{-/-}$ and *p53*$^{-/-}$ mice to IR (5 Gy). (**B**) Quantitation of p53 abundance 4 h after exposure of *Chk2*$^{+/+}$ or *Chk2*$^{-/-}$ thymocytes to IR as in (A). Data are expressed as fold induction relative to the amount of p53 in non-irradiated cells and are means ± standard deviation of values from five independent experiments. (**C**) Protein levels of p53 in MEFs from *Chk2*$^{+/+}$ or *Chk2*$^{-/-}$ mice harvested at the indicated times after 10 Gy IR. (**D**) Effect of expression of recombinant human Chk2 on the IR-induced stabilization of p53 in *Chk2*$^{-/-}$ ES cells. (**E**) Stabilization of p53 protein after IR is dependent on a caffeine-sensitive pathway in *Chk2*$^{-/-}$ cells. *Chk2*$^{+/+}$ and *Chk2*$^{-/-}$ ES cells were pre-treated with or without 5 mM caffeine for 1 h and cell lysates were made 2 h after IR. (**F**) Activation of Chk1 in response to IR. Immunoblot analysis of the time course of Chk1 and Ser345-phosphorylated Chk1 in *Chk2*$^{+/+}$ or *Chk2*$^{-/-}$ MEFs after IR (10 Gy) or UV irradiation (50 J/m^2).

thymocytes (Figure 6A). Similarly, increased mRNA levels for *Mdm2*, *Cdkn1a*, *Pmaip1* and *Ccng* were not observed in *Chk2*$^{-/-}$ MEFs after IR in contrast with *Chk2*$^{+/+}$ MEFs (Figure 6B). Thus, although IR induces stabilization of p53 (albeit to a reduced extent) in *Chk2*$^{-/-}$ cells, the transcriptional activity of p53 is impaired, suggesting that Chk2 is required for the transcriptional activation of p53 by IR.

Phosphorylation and acetylation of p53 in Chk2$^{-/-}$ *ES cells following IR*

Phosphorylation and acetylation are important for stabilizing and activating p53 as a transcription factor (Appella and Anderson, 2001). Since Chk2 is required for IR-induced p53 transcriptional activation (Figure 6), we investigated whether various Ser residues of p53 are phosphorylated in *Chk2*$^{-/-}$ ES cells in response to IR. Immunoblot analysis revealed that IR induced a marked increase in the extent of p53 phosphorylation on Ser18, Ser34 and Ser389 (corresponding to Ser15, Ser33 and Ser392, respectively, in human p53 protein) in both *Chk2*$^{+/+}$ and *Chk2*$^{-/-}$ cells (Figure 7A). Furthermore, Ser23 of mouse p53 (corresponding to Ser20 in human p53) was phosphorylated in both *Chk2*$^{+/+}$ and *Chk2*$^{-/-}$ cells in response to IR, although the signal for phospho-Ser23 was weak. Thus, with regard to the residues examined, the effect of IR on the phosphorylation status of p53 in *Chk2*$^{-/-}$ cells was similar to that in *Chk2*$^{+/+}$ cells (Figure 7A). To eliminate the possibility that the signals detected after IR by our phospho-specific antibodies were due to a larger amount of p53 protein, the phosphorylation status of p53 in ES cells treated with *N*-acetyl-Leu-Leu norleucinal (LLnL), a proteasome inhibitor that stabilizes p53, was examined; however, no phosphorylation on Ser18, Ser23 or Ser34 was observed, indicating that these phosphorylations were induced specifically by DNA damage (Figure 7B). Given that human Chk2 phosphorylates human p53 on Ser20 *in vitro* (Hirao *et al*., 2000; Shieh *et al*., 2000), it seems that the effect of Chk2 on human p53 differs from that on mouse p53. To clarify this possibility, we analyzed the level and phosphorylation status of human p53 in *Chk2*$^{+/+}$ and *Chk2*$^{-/-}$ MEFs using a recombinant, human p53, adenovirus expression vector (Ad-p53). IR induced a slight stabilization of the human p53, and importantly, phosphorylation of Ser15 and Ser20 of human p53 was induced by IR in both *Chk2*$^{+/+}$ and *Chk2*$^{-/-}$ MEFs (Figure 7C). These results indicate that Chk2 is not required for phosphorylation of Ser20 of p53 in either human or mouse cells, and suggest that phosphorylation of Ser20 also is not required for p53 of stabilization.

Acetylation of p53 activates the sequence-specific DNA binding ability of p53 (Appella and Anderson, 2001). Consistent with these notions, Lys379 of mouse p53 was clearly acetylated in response to IR in both *Chk2*$^{+/+}$ and *Chk2*$^{-/-}$ cells, and the acetylated p53 bound the *GADD45A* recognition element (Figure 7D; Supplementary figure 3). UV-induced stabilization of p53 is thought to be Chk2 independent (Hirao *et al*., 2000). Consistent with this notion, equivalent levels of acetylated p53 protein were

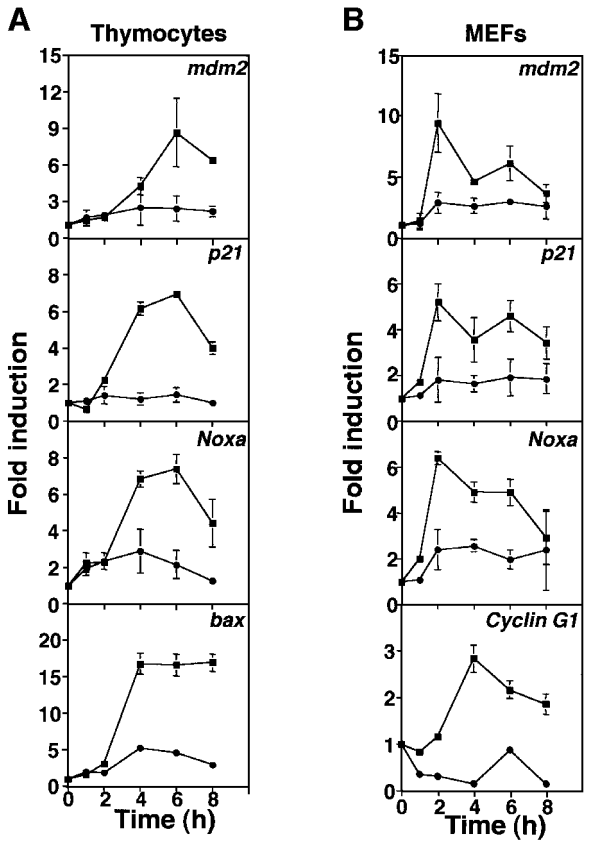

Fig. 6. Defective induction of p53-regulated genes. The fold induction of mRNAs of p53-regulated genes in thymocytes (**A**) and MEFs (**B**) from *Chk2*$^{+/+}$ (squares) and *Chk2*$^{-/-}$ (circles) mice in response to IR. Real-time, quantitative RT–PCR analyses of the expression of *Cdkn1a* (p21), *Pmaip1* (Noxa), *Ccng* (cyclin G1), *Mdm2* and *Bax* following 5 or 10 Gy of IR in *Chk2*$^{+/+}$ or *Chk2*$^{-/-}$ thymocytes or MEFs, respectively. Expression levels of *Gapd* (GAPDH) were monitored as an internal control, and data were normalized to *Gapd* levels. The data are expressed as fold induction by IR and are means ± standard deviation from three independent experiments.

observed after UV irradiation in both *Chk2*$^{+/+}$ and *Chk2*$^{-/-}$ ES cells (Figure 7D).

Discussion

Chk1 and Chk2 are the main effector kinases involved in DNA damage checkpoint control. Mammalian Chk1 is essential for cell growth and early embryonic development in mice (Liu *et al*., 2000; Takai *et al*., 2000). The Chk2 protein kinase, which is activated in response to IR in an ATM-dependent manner, has been implicated in regulating cell cycle arrest at the G_1 checkpoint through phosphorylation of p53 on Ser20 (Chehab *et al*., 2000). Nevertheless, the role of Chk2 in mediating activation of the G_1 checkpoint through p53 stabilization and activation has remained controversial. Phosphorylation of Ser20 failed to block the interaction of p53 with Mdm2 in a direct binding assay (Dumaz and Meek, 1999; Sakaguchi *et al*., 2000). Although changing Ser20 of human p53 to alanine (Ala) was reported recently to make p53 hypersensitive to Mdm2-mediated degradation (Dumaz *et al*., 2001), changing Ser23 of murine p53 to Ala failed to abrogate p53 accumulation or function as a transcription factor in response to IR in murine ES cells, MEFs and thymocytes (Wu *et al*., 2002). Nevertheless, it was reported that *Chk2*$^{-/-}$ ES cells failed to accumulate p53 in response to IR and were defective for p53-dependent transcriptional activation (Hirao *et al*., 2000). Therefore, to further characterize the role of Chk2 in cell cycle responses, we created Chk2-deficient mice by targeted disruption of the *Chk2* gene, and, in contrast to *Chk1*$^{-/-}$ mice, we found that *Chk2*$^{-/-}$ mice are viable and grow normally. However, *Chk2*$^{-/-}$ mice were more resistant than wild-type mice to sublethal doses of IR, and thymocytes and the splenic lymphocytes of *Chk2*$^{-/-}$ mice were resistant to IR-induced apoptosis.

In the response to DNA double-strand breaks, Chk2 is activated through a signaling pathway that depends on ATM (Bartek *et al*., 2001). One of the most striking characteristics of *Atm*$^{-/-}$ mice is acute radiation sensitivity due to gut toxicity (Barlow *et al*., 1996); however, *Chk2*$^{-/-}$ mice show no histological abnormality in the gastrointestinal tract (Figure 1B and C). Thus, Chk2 deficiency is unlikely to play a role in acute radiation toxicity. Splenic lymphocytes of *Chk2*$^{-/-}$ mice exhibited radioresistance (Figure 1D and E), which is also a characteristic of *p53*$^{-/-}$ mice (Westphal *et al*., 1998), and both thymocytes and neurons of the developing brain were resistant to IR-induced apoptosis in *Chk2*$^{-/-}$ mice (Figure 2). IR-induced apoptosis of thymocytes is dependent on p53 (Clarke *et al*., 1993; Lowe *et al*., 1993) but not on ATM (Barlow *et al*., 1997; Herzog *et al*., 1998), whereas IR-induced apoptosis of neurons in the hippocampal dentate gyrus and in the external granule layer of the cerebellum depends on both p53 and ATM (Herzog *et al*., 1998). Furthermore, IR-induced apoptosis of post-mitotic neurons in the neuroepithelial subventricular zone of the developing nervous system during embryogenesis depends on both p53 and ATM, whereas sensitivity of the multipotent precursor cells residing in the proliferating ventricular zone depends only on p53 and not on ATM (Lee *et al*., 2001). Together with our present results, the above observations suggest the existence of ATM-dependent and -independent pathways of Chk2 activation that lead to apoptosis; however, Chk2 appears to be essential for IR-induced apoptosis mediated by p53.

Chk2 acts downstream of ATM and has been implicated in IR-induced cell cycle checkpoint activation by phosphorylating several proteins including Cdc25C, Cdc25A, BRCA1 and p53 (Bartek *et al*., 2001). Chk2 has been thought to contribute to activation of the G_2 checkpoint by IR through phosphorylation of Cdc25C on Ser216, resulting in nuclear export of Cdc25C in association with 14-3-3. Although Hirao *et al*. (2000) reported that Chk2 is required for maintenance of the G_2 arrest in response to IR, we did not observe a defect in either initiation or maintenance of the G_2 arrest in *Chk2*$^{-/-}$ MEFs or ES cells (Figure 3). Chk2 may affect p53-independent initiation of G_1 and S phase checkpoints in response to IR through phosphorylating Cdc25A on Ser123, which induces destruction of Cdc25A and thereby inhibits cyclin E-associated Cdk2 activity (Bartek *et al*., 2001). The activity of cyclin E-associated Cdk2 clearly decreased in response to IR in *Chk2*$^{-/-}$ MEFs (Figure 4G and H), although the response may be slightly delayed in *Chk2*$^{-/-}$ MEFs (Figure 4H, 0.5 h sample). Inhibition of DNA

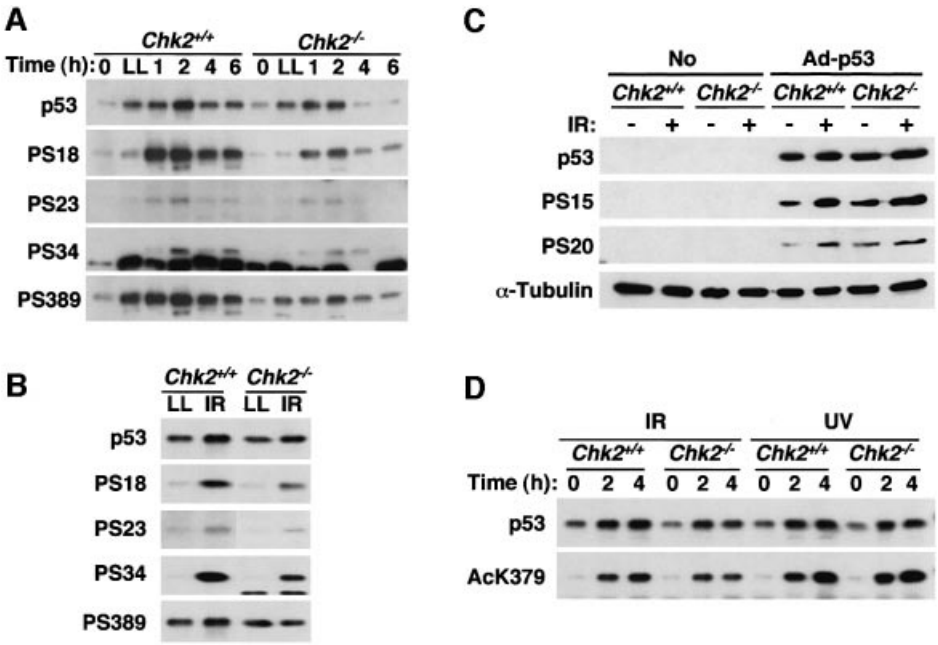

Fig. 7. Phosphorylation and acetylation of p53 protein in *Chk2*$^{-/-}$ cells after IR. (**A**) ES cells were exposed to 10 Gy IR or treated with 10 μM of LLnL (LL) and then lysed at the indicated times after treatment. Immunoprecipitates prepared with PAb421 were subjected to immunoblot analysis with the p53-specific antibodies PAb421 and PAb240 (p53) or with antibodies specific for p53 phosphorylated on the indicated serine residues (PS18, PS23, PS34 or PS389). (**B**) Similar amounts of p53 protein from irradiated or LLnL (LL)-treated ES cells harvested 2 or 4 h after treatment, respectively, were subjected to immunoblot analysis of p53 as in (A). (**C**) *Chk2*$^{+/+}$ and *Chk2*$^{-/-}$ MEFs infected with or without adenovirus-expressing human p53 were cultured for 24 h, the cells were exposed (or not) to 10 Gy IR and then lysed 2 h after IR. Total cell lysates were analyzed by immunoblot using either the human p53-specific monoclonal antibodiy DO-1 (p53), phosphoserine-specific antibodies [anti-human p53 PabSer(P)15 (PS15) and anti-PAb(P)20 (PS20)] or anti-α-tubulin as probes. (**D**) Differentiated ES cells were exposed to IR (10 Gy) or UV light (50 J/m^2) and lysed at the indicated times after treatment. Immunoprecipitates prepared with PAb421 antibodies were subject to immunoblot analysis with p53-specific PAb421 and PAb240 or with antibodies specific for p53 acetylated on lysine379 (AcK379).

synthesis did occur and an enhanced G_2/M accumulation, a consequence of a defective S phase checkpoint (Xu *et al*., 2002), was not observed in *Chk2*$^{-/-}$ MEFs (Figures 3C, D and 4F). These results suggest that Chk2 is not essential for p53-independent initiation of G_1 and S phase checkpoints in response to IR. However, the inhibition of DNA synthesis in *Chk2*$^{-/-}$ MEFs was slightly less than that in *Chk2*$^{+/+}$ MEFs (Figure 4F), raising the possibility that the absence of Chk2 may be compensated by other pathways such as through Chk1 (see below). Chk2 also phosphorylates BRCA1 on Ser988, which may be required for resistance to IR. Cells deficient in BRCA1 have defects in the S and G_2 checkpoint responses to IR (Xu *et al*., 2001), and they are sensitive to various DNA damaging stimuli (Gowen *et al*., 1998). As we demonstrated that viability of *Chk2*$^{-/-}$ ES cells to various DNA damaging stimuli was comparable to that of *Chk2*$^{+/+}$ ES cells (Supplementary figure 2), Chk2 might be dispensable for the function of BRCA1. A recent report shows that BRCA1 regulates the G_2/M checkpoint by activating Chk1 after IR (Yarden *et al*., 2002). As Chk1 phosphorylates Cdc25A and Cdc25C (Sanchez *et al*., 1997; Mailand *et al*., 2000), it may compensate for Chk2 deficiency to activate p53-independent initiation of the G_1, S phase and G_2 checkpoints in *Chk2*$^{-/-}$ cells. Indeed, Chk1 was rapidly activated in both *Chk2*$^{+/+}$ and *Chk2*$^{-/-}$ MEFs in response to IR (Figure 5F).

Chehab *et al*. (2000) showed that human Chk2 functions in the G_1 arrest in response to IR through p53. Consistent with this notion, we have now shown that Chk2 is necessary for efficient p53-dependent G_1 arrest in response to IR (Figure 5A–E). *Chk2*$^{-/-}$ MEFs thus were markedly deficient in their ability to maintain a G_1 arrest in response to IR. This characteristic of *Chk2*$^{-/-}$ MEFs is similar to that of *Cdkn1a*$^{-/-}$ (p21-deficient) MEFs (Brugarolas *et al*., 1995; Deng *et al*., 1995). These observations also are consistent with our data showing that the IR-induced increase in the abundance of p21 mRNA was impaired in *Chk2*$^{-/-}$ thymocytes and MEFs (Figure 6), that the activity of cyclin E-associated Cdk2 again increased by 2.5 h after IR in *Chk2*$^{-/-}$ MEFs (Figure 4H) and that p53-dependent maintenance of the G_1 arrest was impaired.

p53 protein stability is regulated by Mdm2, an E3 ligase important for p53 ubiquitylation (Ashcroft *et al*., 1999). Inhibiting the interaction of p53 and Mdm2 after DNA damage through phosphorylation of p53 on N-terminal Ser and Thr residues was suggested to be critical for stabilizing p53 after DNA damage (Appella and Anderson, 2001). Human Chk2 phosphorylates Ser20 of human p53 *in vitro* (Chehab *et al*., 2000; Hirao *et al*., 2000; Shieh *et al*., 2000), and activation of human Chk2 induced the phosphorylation of p53 on Ser20 *in vivo* and triggered the dissociation of Mdm2 from the p53 complex (Chehab *et al*., 2000). Hirao *et al*. (2000) also showed that mouse Chk2 is essential for stabilizing mouse p53 protein in response to IR. However, our results now demonstrate that phosphorylation of p53 at Ser18, Ser23 and Ser34 occurs normally after IR in *Chk2*$^{-/-}$ cells (Figure 7), and the p53 protein clearly was stabilized in response to IR in our *Chk2*$^{-/-}$ ES cells, MEFs and thymocytes (Figure 5).

Furthermore, human p53 was phosphorylated on Ser20 and Ser15 in *Chk2*$^{-/-}$ MEFs in response to IR (Figure 7C). These results suggest that while Chk2 contributes to the stabilization of murine p53, another pathway, perhaps involving Chk1 (see above) or an unidentified kinase(s), partially compensates for the Chk2 deficiency. Chk1, which acts downstream of ATR, or the Polo-like kinase 3 (Plk3), which is activated in an ATM-dependent manner in response to IR, both are able to phosphorylate human p53 on Ser20 *in vitro* (Shieh *et al*., 2000; Xie *et al*., 2001). That ATM and ATR contribute to p53 stabilization after IR through both direct and indirect mechanisms is indicated by several observations. (i) The extent of p53 stabilization in *Chk2*$^{-/-}$ cells was markedly reduced by caffeine treatment (Figure 5E); (ii) Ser395 of Mdm2 is a target for phosphorylation by ATM, a reaction that attenuates the ability of Mdm2 to promote the nuclear export of p53 leading to its degradation (Maya *et al*., 2001); and (iii) ATM and ATR phosphorylate E2F-1 on Ser31, resulting in the accumulation of this transcription factor (Lin *et al*., 2001); the accumulated E2F-1 may have stabilized p53 through inducing p19^{ARF} expression, thereby preventing Mdm2 action.

Whereas IR induced substantial stabilization of p53 in *Chk2*$^{-/-}$ cells (Figure 5), p53-mediated G_1 arrest and apoptosis were markedly impaired (Figures 2 and 4). Target genes of p53, including those for *Cdkn1a* (p21) (which mediates maintenance of G_1), *Pmaip1* (Noxa) and *Bax* (which induce apoptosis), and *Mdm2* and *Ccng* (cyclin G1), were not induced by IR in *Chk2*$^{-/-}$ cells, even in the presence of high concentrations of p53 (Figures 5 and 6). These observations suggest that Chk2 is required for the transcriptional activation of p53 in response to IR. Acetylation of p53 on several C-terminal lysines, including Lys382, is believed to be important for p53 activation (Ito *et al*., 2001; Luo *et al*., 2001; Vaziri *et al*., 2001). In human cells, accumulating evidence indicates that phosphorylation of N-terminal serines, including Ser15, facilitates the acetylation of C-terminal lysines through recruitment of CBP/p300 and PCAF (Lambert *et al*., 1998; Sakaguchi *et al*., 1998). As noted above, we found that Ser18, Ser23, Ser34 and Ser389 (corresponding to human Ser15, Ser20, Ser33 and Ser392) were phosphorylated in *Chk2*$^{-/-}$ cells in response to IR (Figure 7A and B). Consistent with this result, Lys379 (corresponding to human Lys382) was acetylated in *Chk2*$^{-/-}$ cells in response to IR (Figure 7D). Thus, while phosphorylation of Ser18, Ser23, Ser34 and Ser389, and acetylation of Lys379 of murine p53 were sufficient for p53 protein stabilization, these modifications were not sufficient for p53 transcriptional activation. Mutant human p53 that has Ser20 substituted by Ala is still phosphorylated by recombinant human Chk2, indicating that Ser20 may not be the only site phosphorylated by Chk2 *in vivo* (Shieh *et al*., 2000). Alternatively, Chk2 may phosphorylate an unidentified protein that interacts with p53 to regulate its transcriptional activity. Work currently in progress is directed toward addressing these important questions.

In addition to the recently identified heterozygous germline mutations in *Chk2* in a subset of patients with Li–Fraumeni syndrome (Bell *et al*., 1999), mutations in the *Chk2* gene were detected in sporadic colon (Bell *et al*., 1999), lung (Haruki *et al*., 2000) and breast cancers (Meijers-Heijboer *et al*., 2002). During their first year, *Chk2*$^{-/-}$ mice have a low incidence of spontaneous tumor formation; only one of 34 *Chk2*$^{-/-}$ mice developed a tumor, which was of mammary epithelial origin. However, our preliminary observations indicate that *Chk2*$^{-/-}$ mice, but not *Chk2*$^{+/-}$ and *Chk2*$^{+/+}$ mice, develop tumors (e.g. lymphomas) and start to die after 71 weeks. Taken together, our data suggest that Chk2 may function as a tumor suppressor gene. Although activity of the p53 protein is regulated through several pathways, here we demonstrate that Chk2 has pivotal roles in regulating p53 functions after IR treatment. Currently, we are following a cohort of irradiated *Chk2*$^{+/+}$, *Chk2*$^{+/-}$ and *Ch2*$^{-/-}$ mice to determine whether irradiation causes increased tumor frequency in *Chk2*$^{+/-}$ and *Chk2*$^{-/-}$ mice.

Materials and methods

Targeting vector, homologous recombination and animal breeding

Chk2-deficient mice and cells were generated by standard methods as described previously (Kobayashi *et al*., 2002; see Supplementary data).

Ionizing irradiation, tissue preparation and microscopic analysis

Groups of neonatal and 4–16-week-old mice of the indicated genotypes received single exposures of the indicated dose of IR (X-rays). Pathological analyses were performed as described previously (Kobayashi *et al*., 2002).

Cells and culture conditions

Cells were maintained as described previously (Takai *et al*., 2000). *Chk2*$^{-/-}$ ES cells were established from *Chk2*$^{+/-}$ ES cells by cultivating in medium containing a high concentration (3 mg/ml) of G418. The sensitivity of *Chk2*$^{-/-}$ ES cells to X-ray and UV radiation was determined by measuring their colony-forming ability as described previously (Kobayashi *et al*., 2002). Differentiation of ES cells *in vitro* with retinoic acid was performed as described previously (Chao *et al*., 2000). Analyses of thymocytes were described previously (Motoyama *et al*., 1995).

Cell cycle analysis

Mitotic index was measured as described previously (Hirao *et al*., 2000; Xu *et al*., 2001). For cell cycle analysis, replicative DNA synthesis and DNA content were evaluated by two-color flow cytometry according to standard procedures (see Supplementary data).

Recombinant adenovirus encoding human p53 (Ad-p53) was the kind gift of Takashi Tokino (Sapporo Medical University) and was described previously (Ishida *et al*., 2000). MEFs (20 000 cells) in serum-free medium were infected with Ad-p53 at a multiplicity of infection of 100 plaque-forming units/cell. After 1 h, DMEM with 0.1% FBS was added and the cells were incubated for an additional 24 h and then irradiated with X-rays at 10 Gy.

Protein analysis

Cells were lysed as described previously (Takai *et al*., 2000), and lysates or immunoprecipitates were subjected to SDS–PAGE, immunoblot analysis and kinase assay according to standard procedures (see Supplementary data).

Quantitative RT–PCR analysis

Real-time, quantitative PCR was performed on a light cycler (Roche) using LightCycler-FastStart DNA Master SYBR Green I (Roche); then the relative amounts of specifically amplified cDNA were calculated using *Gapd* (GAPDH) as an internal reference according to manufacturers' instructions (see Supplementary data).

Supplementary data

Supplementary data are available at *The EMBO Journal* Online.

Acknowledgements

We thank Bert R.Williams for technical comment, Takashi Tokino for Ad-p53, Yasuko Orba and Mami Satoh for histological analysis and Kumi Tsutsumi, Yoshiko Kondoh, Yayoi Tanaka and Yumi Eto for general technical assistance. Y.O. is a research fellow of the Japan Society for the Promotion of Science. S.S. and C.W.A. were supported in part by a Laboratory Directed Research and Development grant at the Brookhaven National Laboratory under contract with the US Department of Energy. This work was supported in part by a Grant-in-Aid for Scientific Research on Priority Areas (to N.M.) from the Ministry of Education, Science, Sports and Culture of Japan, and by Health Sciences Research Grants for Research on the Comprehensive Research on Aging and Health (to N.M.) and for Human Genome and Gene Therapy (to K.I.) from the Ministry of Health, Labor and Welfare of Japan.

References

Appella,E. and Anderson,C.W. (2001) Post-translational modifications and activation of p53 by genotoxic stresses. *Eur. J. Biochem.*, **268**, 2764–2772.

Ashcroft,M., Kubbutat,M.H. and Vousden,K.H. (1999) Regulation of p53 function and stability by phosphorylation. *Mol. Cell. Biol.*, **19**, 1751–1758.

Banin,S. *et al.* (1998) Enhanced phosphorylation of p53 by ATM in response to DNA damage. *Science*, **281**, 1674–1677.

Barlow,C. *et al.* (1996) *Atm*-deficient mice: a paradigm of ataxia telangiectasia. *Cell*, **86**, 159–171.

Barlow,C., Brown,K.D., Deng,C.X., Tagle,D.A. and Wynshaw-Boris,A. (1997) Atm selectively regulates distinct p53-dependent cell-cycle checkpoint and apoptotic pathways. *Nat. Genet.*, **17**, 453–456.

Bartek,J., Falck,J. and Lukas,J. (2001) CHK2 kinase—a busy messenger. *Nat. Rev. Mol. Cell. Biol.*, **2**, 877–886.

Bell,D.W. *et al.* (1999) Heterozygous germ line *hCHK2* mutations in Li–Fraumeni syndrome. *Science*, **286**, 2528–2531.

Brugarolas,J., Chandrasekaran,C., Gordon,J.I., Beach,D., Jacks,T. and Hannon,G.J. (1995) Radiation-induced cell cycle arrest compromised by p21 deficiency. *Nature*, **377**, 552–557.

Canman,C.E., Lim,D.S., Cimprich,K.A., Taya,Y., Tamai,K., Sakaguchi, K., Appella,E., Kastan,M.B. and Siliciano,J.D. (1998) Activation of the ATM kinase by ionizing radiation and phosphorylation of p53. *Science*, **281**, 1677–1679.

Chao,C., Saito,S., Anderson,C.W., Appella,E. and Xu,Y. (2000) Phosphorylation of murine p53 at ser-18 regulates the p53 responses to DNA damage. *Proc. Natl Acad. Sci. USA*, **97**, 11936–11941.

Chehab,N.H., Malikzay,A., Stavridi,E.S. and Halazonetis,T.D. (1999) Phosphorylation of Ser-20 mediates stabilization of human p53 in response to DNA damage. *Proc. Natl Acad. Sci. USA*, **96**, 13777–13782.

Chehab,N.H., Malikzay,A., Appel,M. and Halazonetis,T.D. (2000) Chk2/hCds1 functions as a DNA damage checkpoint in G_1 by stabilizing p53. *Genes Dev.*, **14**, 278–288.

Clarke,A.R., Purdie,C.A., Harrison,D.J., Morris,R.G., Bird,C.C., Hooper,M.L. and Wyllie,A.H. (1993) Thymocyte apoptosis induced by p53-dependent and independent pathways. *Nature*, **362**, 849–852.

Deng,C., Zhang,P., Harper,J.W., Elledge,S.J. and Leder,P. (1995) Mice lacking $p21^{CIP1/WAF1}$ undergo normal development, but are defective in G_1 checkpoint control. *Cell*, **82**, 675–684.

Dumaz,N. and Meek,D.W. (1999) Serine15 phosphorylation stimulates p53 transactivation but does not directly influence interaction with HDM2. *EMBO J.*, **18**, 7002–7010.

Dumaz,N., Milne,D.M., Jardine,L.J. and Meek,D.W. (2001) Critical roles for the serine 20, but not the serine 15, phosphorylation site and for the polyproline domain in regulating p53 turnover. *Biochem. J.*, **359**, 459–464.

Giaccia,A.J. and Kastan,M.B. (1998) The complexity of p53 modulation: emerging patterns from divergent signals. *Genes Dev.*, **12**, 2973–2983.

Gowen,L.C., Avrutskaya,A.V., Latour,A.M., Koller,B.H. and Leadon, S.A. (1998) BRCA1 required for transcription-coupled repair of oxidative DNA damage. *Science*, **281**, 1009–1012.

Haruki,N., Saito,H., Tatematsu,Y., Konishi,H., Harano,T., Masuda,A., Osada,H., Fujii,Y. and Takahashi,T. (2000) Histological type-selective, tumor-predominant expression of a novel *CHK1* isoform and infrequent *in vivo* somatic *CHK2* mutation in small cell lung cancer. *Cancer Res.*, **60**, 4689–4692.

Herzog,K.H., Chong,M.J., Kapsetaki,M., Morgan,J.I. and McKinnon,P.J. (1998) Requirement for Atm in ionizing radiation-induced cell death in the developing central nervous system. *Science*, **280**, 1089–1091.

Hirao,A., Kong,Y.Y., Matsuoka,S., Wakeham,A., Ruland,J., Yoshida,H., Liu,D., Elledge,S.J. and Mak,T.W. (2000) DNA damage-induced activation of p53 by the checkpoint kinase Chk2. *Science*, **287**, 1824–1827.

Ishida,S., Yamashita,T., Nakaya,U. and Tokino,T. (2000) Adenovirus-mediated transfer of p53-related genes induces apoptosis of human cancer cells. *Jpn J. Cancer Res.*, **91**, 174–180.

Ito,A., Lai,C.H., Zhao,X., Saito,S., Hamilton,M.H., Appella,E. and Yao,T.P. (2001) p300/CBP-mediated p53 acetylation is commonly induced by p53-activating agents and inhibited by MDM2. *EMBO J.*, **20**, 1331–1340.

Kastan,M.B. and Lim,D.S. (2000) The many substrates and functions of ATM. *Nat. Rev. Mol. Cell. Biol.*, **1**, 179–186.

Kobayashi,Y. *et al.* (2002) Hydrocephalus, situs inversus, chronic sinusitis, and male infertility in DNA polymerase λ-deficient mice: possible implication for the pathogenesis of immotile cilia syndrome. *Mol. Cell. Biol.*, **22**, 2769–2776.

Lambert,P.F., Kashanchi,F., Radonovich,M.F., Shiekhattar,R. and Brady,J.N. (1998) Phosphorylation of p53 serine 15 increases interaction with CBP. *J. Biol. Chem.*, **273**, 33048–33053.

Lee,Y., Chong,M.J. and McKinnon,P.J. (2001) Ataxia telangiectasia mutated-dependent apoptosis after genotoxic stress in the developing nervous system is determined by cellular differentiation status. *J. Neurosci.*, **21**, 6687–6693.

Liang,S.H. and Clarke,M.F. (2001) Regulation of p53 localization. *Eur. J. Biochem.*, **268**, 2779–2783.

Lin,W.C., Lin,F.T. and Nevins,J.R. (2001) Selective induction of E2F1 in response to DNA damage, mediated by ATM-dependent phosphorylation. *Genes Dev.*, **15**, 1833–1844.

Liu,Q. *et al.* (2000) Chk1 is an essential kinase that is regulated by Atr and required for the G_2/M DNA damage checkpoint. *Genes Dev.*, **14**, 1448–1459.

Lowe,S.W., Schmitt,E.M., Smith,S.W., Osborne,B.A. and Jacks,T. (1993) p53 is required for radiation-induced apoptosis in mouse thymocytes. *Nature*, **362**, 847–849.

Luo,J., Nikolaev,A.Y., Imai,S., Chen,D., Su,F., Shiloh,A., Guarente,L. and Gu,W. (2001) Negative control of p53 by Sir2α promotes cell survival under stress. *Cell*, **107**, 137–148.

Mailand,N., Falck,J., Lukas,C., Syljuåsen,R.G., Welcker,M., Bartek,J. and Lukas,J. (2000) Rapid destruction of human Cdc25A in response to DNA damage. *Science*, **288**, 1425–1429.

Maya,R. *et al.* (2001) ATM-dependent phosphorylation of Mdm2 on serine 395: role in p53 activation by DNA damage. *Genes Dev.*, **15**, 1067–1077.

Meijers-Heijboer,H. *et al.* (2002) Low-penetrance susceptibility to breast cancer due to *CHEK2**1100delC in noncarriers of BRCA1 or BRCA2 mutations. *Nat. Genet.*, **31**, 55–59.

Motoyama,N. *et al.* (1995) Massive cell death of immature hematopoietic cells and neurons in Bcl-x-deficient mice. *Science*, **267**, 1506–1510.

Prives,C. and Hall,P.A. (1999) The p53 pathway. *J. Pathol.*, **187**, 112–126.

Rotman,G. and Shiloh,Y. (1999) ATM: a mediator of multiple responses to genotoxic stress. *Oncogene*, **18**, 6135–6144.

Sakaguchi,K., Herrera,J.E., Saito,S., Miki,T., Bustin,M., Vassilev,A., Anderson,C.W. and Appella,E. (1998) DNA damage activates p53 through a phosphorylation-acetylation cascade. *Genes Dev.*, **12**, 2831–2841.

Sakaguchi,K., Saito,S., Higashimoto,Y., Roy,S., Anderson,C.W. and Appella,E. (2000) Damage-mediated phosphorylation of human p53 threonine 18 through a cascade mediated by a casein 1-like kinase. Effect on Mdm2 binding. *J. Biol. Chem.*, **275**, 9278–9283.

Sanchez,Y., Wong,C., Thoma,R.S., Richman,R., Wu,Z., Piwnica-Worms,H. and Elledge,S.J. (1997) Conservation of the Chk1 checkpoint pathway in mammals: linkage of DNA damage to Cdk regulation through Cdc25. *Science*, **277**, 1497–1501.

Sarkaria,J.N., Busby,E.C., Tibbetts,R.S., Roos,P., Taya,Y., Karnitz,L.M. and Abraham,R.T. (1999) Inhibition of ATM and ATR kinase activities by the radiosensitizing agent, caffeine. *Cancer Res.*, **59**, 4375–4382.

Shieh,S.Y., Ikeda,M., Taya,Y. and Prives,C. (1997) DNA damage-induced phosphorylation of p53 alleviates inhibition by MDM2. *Cell*, **91**, 325–334.

Shieh,S.Y., Ahn,J., Tamai,K., Taya,Y. and Prives,C. (2000) The human

homologs of checkpoint kinases Chk1 and Cds1 (Chk2) phosphorylate p53 at multiple DNA damage-inducible sites. *Genes Dev.*, **14**, 289–300.

Takai,H. *et al.* (2000) Aberrant cell cycle checkpoint function and early embryonic death in *Chk1*$^{-/-}$ mice. *Genes Dev.*, **14**, 1439–1447.

Vaziri,H., Dessain,S.K., Ng Eaton,E., Imai,S.I., Frye,R.A., Pandita,T.K., Guarente,L. and Weinberg,R.A. (2001) *hSIR2*^{SIRT1} functions as an NAD-dependent p53 deacetylase. *Cell*, **107**, 149–159.

Vousden,K.H. (2000) p53: death star. *Cell*, **103**, 691–694.

Westphal,C.H., Hoyes,K.P., Canman,C.E., Huang,X., Kastan,M.B., Hendry,J.H. and Leder,P. (1998) Loss of atm radiosensitizes multiple p53 null tissues. *Cancer Res.*, **58**, 5637–5639.

Wu,Z., Earle,J., Saito,S., Anderson,C.W., Appella,E. and Xu,Y. (2002) Mutation of mouse p53 Ser23 and the response to DNA damage. *Mol. Cell. Biol.*, **22**, 2441–2449.

Xie,S., Wang,Q., Wu,H., Cogswell,J., Lu,L., Jhanwar-Uniyal,M. and Dai,W. (2001) Reactive oxygen species-induced phosphorylation of p53 on serine 20 is mediated in part by polo-like kinase-3. *J. Biol. Chem.*, **276**, 36194–36199.

Xu,B., Kim,S. and Kastan,M.B. (2001) Involvement of Brca1 in S-phase and G_2-phase checkpoints after ionizing irradiation. *Mol. Cell. Biol.*, **21**, 3445–3450.

Xu,B., Kim,S.T., Lim,D.S. and Kastan,M.B. (2002) Two molecularly distinct G_2/M checkpoints are induced by ionizing irradiation. *Mol. Cell. Biol.*, **22**, 1049–1059.

Yarden,R.I., Pardo-Reoyo,S., Sgagias,M., Cowan,K.H. and Brody,L.C. (2002) BRCA1 regulates the G_2/M checkpoint by activating Chk1 kinase upon DNA damage. *Nat. Genet.*, **30**, 285–289.

Received January 4, 2002; revised August 1, 2002; accepted August 5, 2002